Expanded View Figures

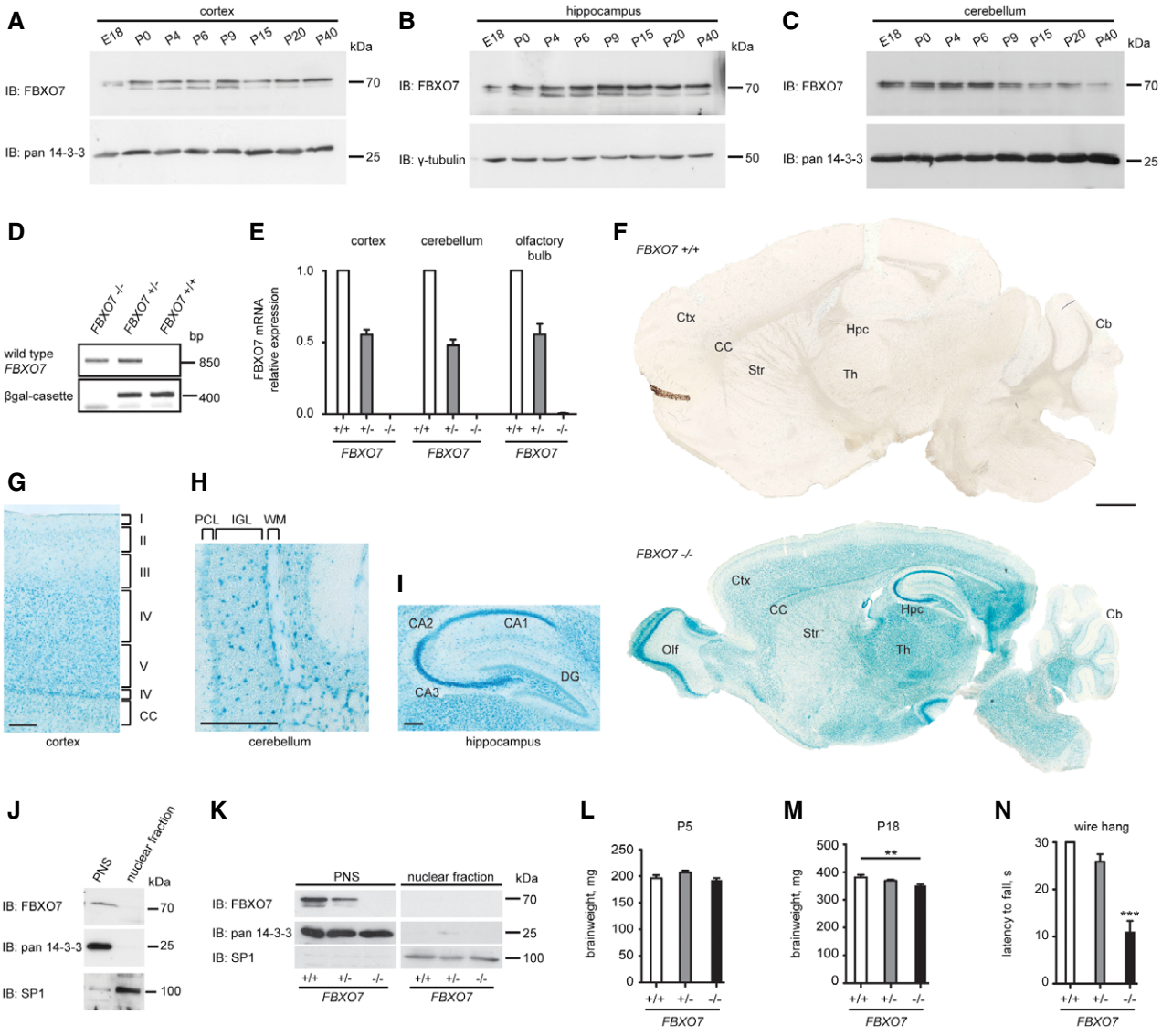

Figure EV1. Characterization of *FBXO7*$^{-/-}$ mice.

A–C Lysates of cortices (A), hippocampi (B), and cerebella (C) of the indicated age isolated from rat were immunoblotted with FBXO7, pan 14-3-3, or γ-tubulin antibodies. The latter two served as loading controls.

D Genotyping of *FBXO7*$^{+/+}$, *FBXO7*$^{+/-}$, and *FBXO7*$^{-/-}$ mice. Detection of wild-type and mutant *FBXO7* alleles.

E Quantitative PCR of *FBXO7*$^{+/+}$, *FBXO7*$^{+/-}$ and *FBXO7*$^{-/-}$ brain tissue. n = 4, 2, and 4, respectively (mean ± s.e.m.).

F LacZ staining of P18 *FBXO7*$^{+/+}$ and *FBXO7*$^{-/-}$ sagittal brain sections. Ctx = cortex, Hpc = hippocampus, Cb = cerebellum, Olf = olfactory bulb, CC = corpus callosum, Str = striatum, Th = thalamus. Scale bar = 1 mm.

G–I Higher magnification of LacZ-stained P18 *FBXO7*$^{-/-}$ sagittal brain: cortex (G), cerebellum (H), and hippocampus (I). CC = corpus callosum, PCL = Purkinje cell layer, IGL = internal granule cell layer, WM = white matter, DG = dentate gyrus, CA1, 2, 3 = cornus ammonis 1, 2, 3. Scale bars = 200 μm.

J, K Cultured rat cerebellar granule neurons (J) or mouse cortical tissue (K) was subjected to subcellular fractionation analyses. Nuclear fraction and postnuclear supernatant (PNS) were immunoblotted with FBXO7, SP1, and pan 14-3-3 antibodies. The latter two served as quality control for the nuclear fraction and PNS, respectively.

L, M Brain weight of P5 and P18 *FBXO7*$^{+/+}$, *FBXO7*$^{+/-}$, or *FBXO7*$^{-/-}$ mice. n = 8, 20, and 7 (L) and n = 6, 11, and 8 (M), respectively (ANOVA, $^{**}P < 0.01$, mean ± s.e.m.).

N P18 littermates were tested on the hanging wire. n = 20, 23, and 16, respectively (ANOVA, $^{***}P < 0.001$, mean ± s.e.m.).

Source data are available online for this figure.

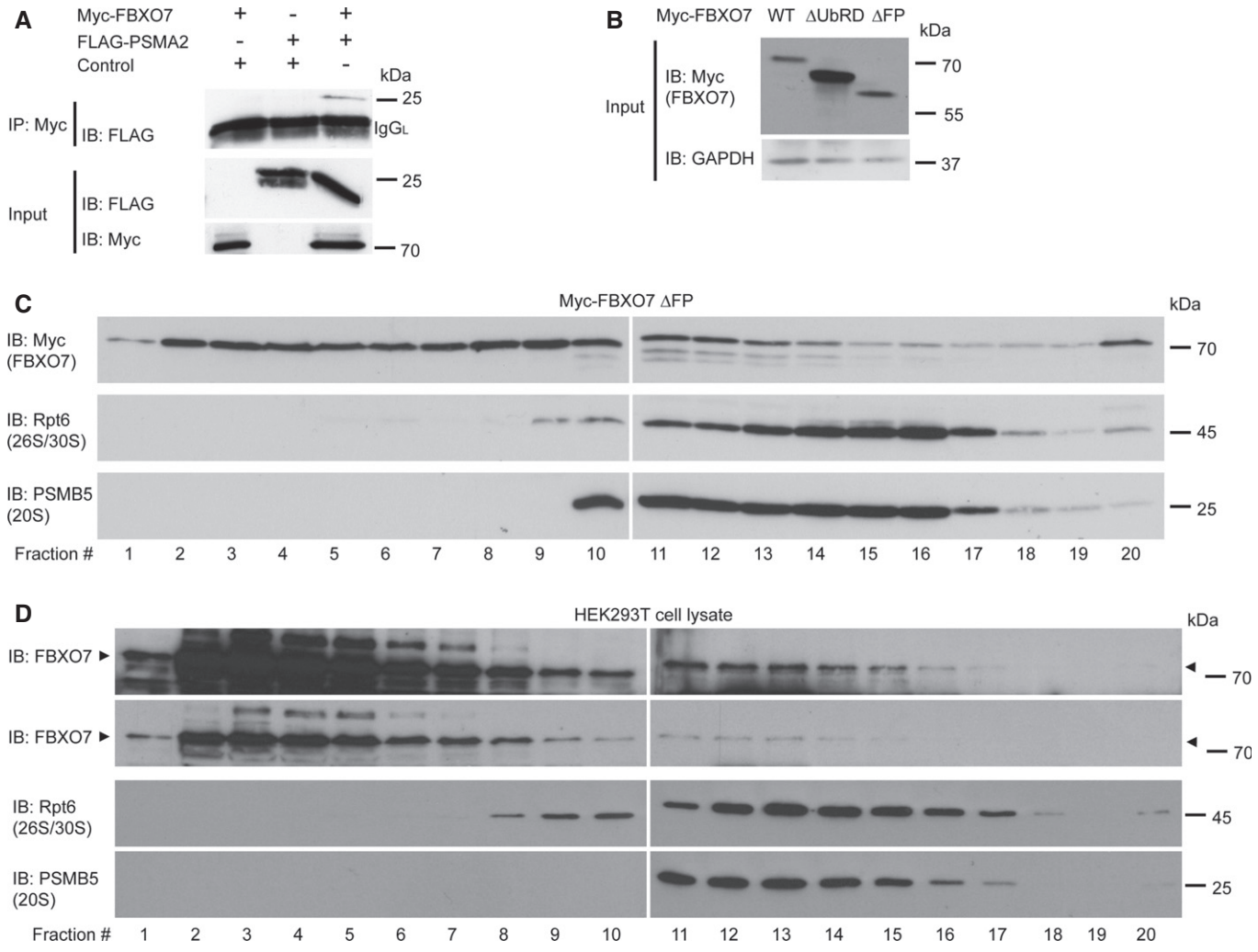

Figure EV2. FBXO7 interacts with the proteasomal subunit PSMA2 and binds to the proteasome.

A Lysates of HEK293T cells, transfected with the indicated plasmids, were subjected to IP with myc antibody for FBXO7, followed by IB with FLAG antibody for PSMA2.

B Input from HEK293T cells, transfected with full-length myc-FBXO7, ΔUbRD, or ΔFP (panel C and Fig 3E), was immunoblotted with myc (FBXO7) or GAPDH antibody. The latter served as a loading control.

C HEK293T cells were transfected with myc-FBXO7 ΔFP and subjected to fractionation using a 10–40% linear glycerol gradient. Fractions were immunoblotted for myc (FBXO7), Rpt6 (26S/30S proteasome), and PSMB5 (20S proteasome).

D HEK293T cells were subjected to fractionation using a 10–40% linear glycerol gradient. Fractions were immunoblotted for FBXO7, Rpt6 (26S/30S proteasome), and PSMB5 (20S proteasome).

Source data are available online for this figure.

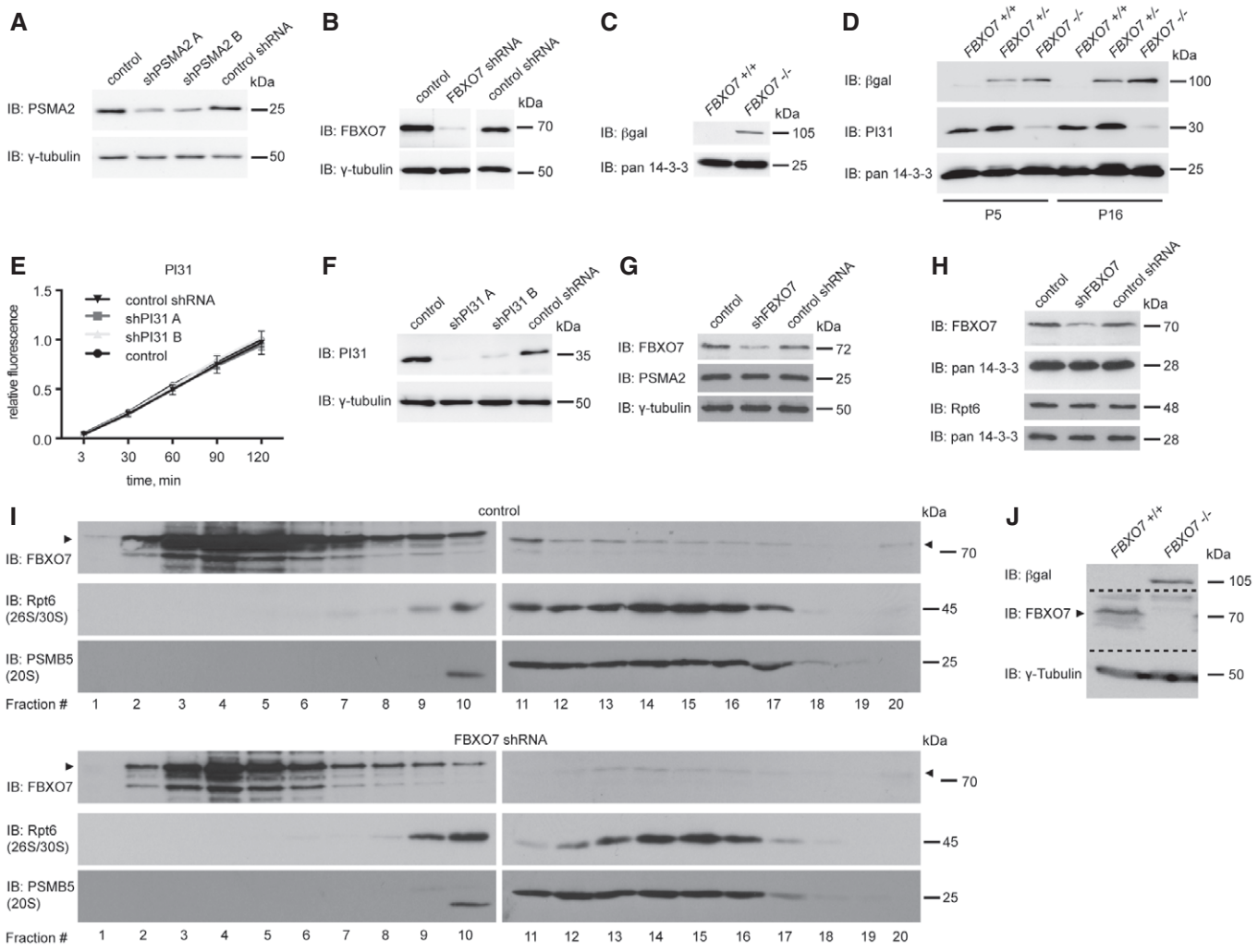

Figure EV3. FBXO7 ubiquitinates PSMA2 and regulates proteasome assembly.

A Control of knockdown for Fig 5A. Lysates of HEK293T cells transfected with empty control vector or PSMA2 shRNA plasmids were immunoblotted with PSMA2 or γ-tubulin antibody. The latter served as a loading control.

B Control of knockdown for Fig 5B. Lysates of HEK293T cells transfected with empty control vector, FBXO7 shRNA, or non-functional FBXO7 shRNA plasmids, were immunoblotted with FBXO7 or γ-tubulin antibody. The latter served as a loading control.

C Control of knockout for Fig 5C. Brain lysates from *FBXO7*$^{+/+}$ or *FBXO7*$^{-/-}$ mice were immunoblotted with βgal or pan 14-3-3 antibody. The latter served as a loading control.

D Whole brain lysates from *FBXO7*$^{+/+}$, *FBXO7*$^{+/-}$, and *FBXO7*$^{-/-}$ mice at age P5 and P16 were subjected to immunoblotting with βgal and PI31 antibodies. Pan 14-3-3 was used as a loading control.

E Lysates from HEK293T cells, transfected with empty control vector, functional PI31 shRNA, or non-functional PI31 shRNA, were analyzed for chymotrypsin-like proteasome activity assay (LLVY-AMC). Three independent experiments were carried out (ANOVA, mean ± s.e.m.).

F Input from (E) was immunoblotted with PI31 or γ-tubulin antibody. The latter served as a loading control.

G Control of knockdown and loading for Fig 5E. Lysates of HEK293T cells transfected with empty control vector or FBXO7 shRNA plasmids were immunoblotted with FBXO7, PSMA2, or γ-tubulin antibody. The latter served as a loading control.

H Control of knockdown and loading for Fig 5F. Lysates of HEK293T cells transfected with empty control vector or FBXO7 shRNA plasmids were immunoblotted with FBXO7, Rpt6, or pan14-3-3 antibody. The latter served as a loading control.

I HEK293T cells transfected with empty control vector or the FBXO7 RNAi plasmid were subjected to fractionation using a 10–40% linear glycerol gradient. Fractions were subjected to immunoblotting with FBXO7, Rpt6 (26S/30S proteasome), or PSMB5 (20S proteasome) antibody.

J Control of knockout and loading for Fig 5H. Brain lysates from *FBXO7*$^{+/+}$ or *FBXO7*$^{-/-}$ mice were immunoblotted with βgal, FBXO7, or γ-tubulin antibody. The latter served as loading control.

Source data are available online for this figure.

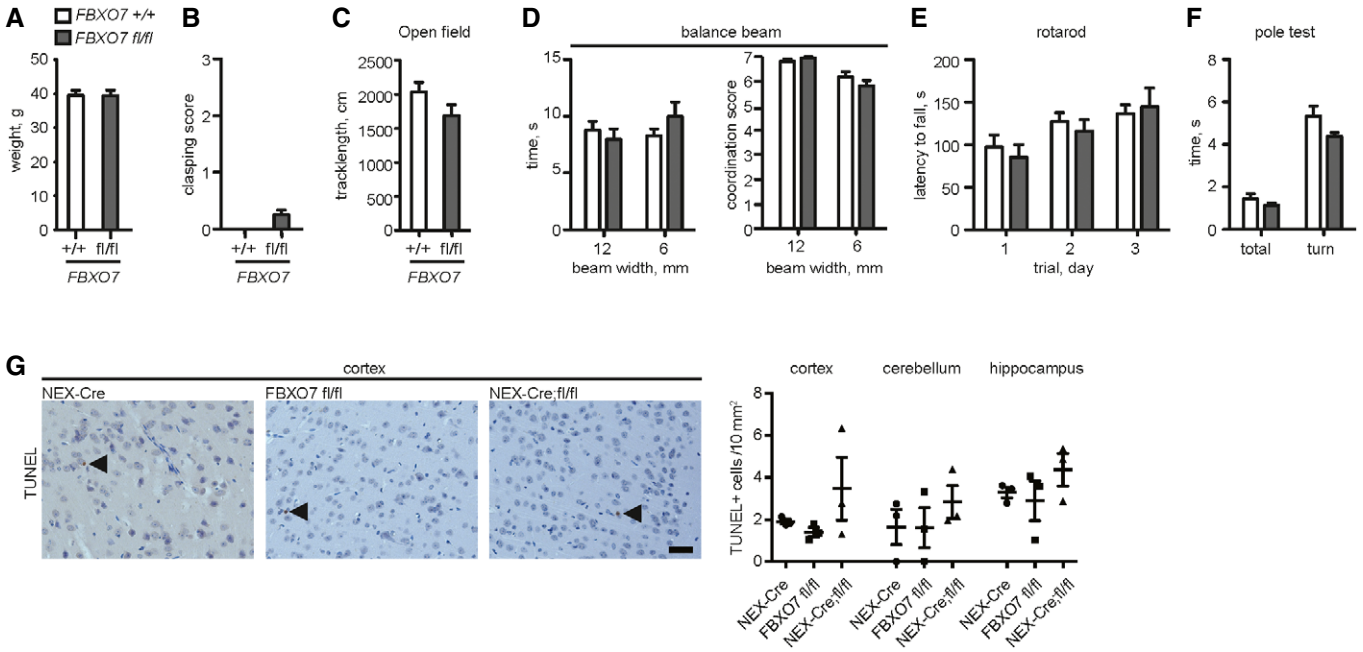

Figure EV4. Deletion of *FBXO7* in the forebrain triggers early-onset motor impairment.

A Average body weight of 12-month-old *FBXO7*$^{+/+}$ or *FBXO7*$^{fl/fl}$ mice. n = 13 and 10, respectively (t-test, mean ± s.e.m.).

B Hind limb clasping of 12-month-old *FBXO7*$^{+/+}$ or *FBXO7*$^{fl/fl}$ mice. n = 13 and 10, respectively (Mann–Whitney U-test, mean ± s.e.m.).

C–F Open field test (C), balance beam test (time to cross and coordination score were measured, D), rotarod (E), and pole test (F) of 12-month-old *FBXO7*$^{+/+}$ or *FBXO7*$^{fl/fl}$ mice. n = 13 and 10, respectively (unpaired t-test or Mann–Whitney U-test (coordination score), mean ± s.e.m.).

G Sagittal paraffin sections from NEX-Cre, *FBXO7*$^{fl/fl}$, or NEX-Cre;fl/fl mice cortices were subjected to TUNEL staining. Three mice per genotype were included in the analysis (ANOVA, mean ± s.e.m.). Scale bar = 40 μm.

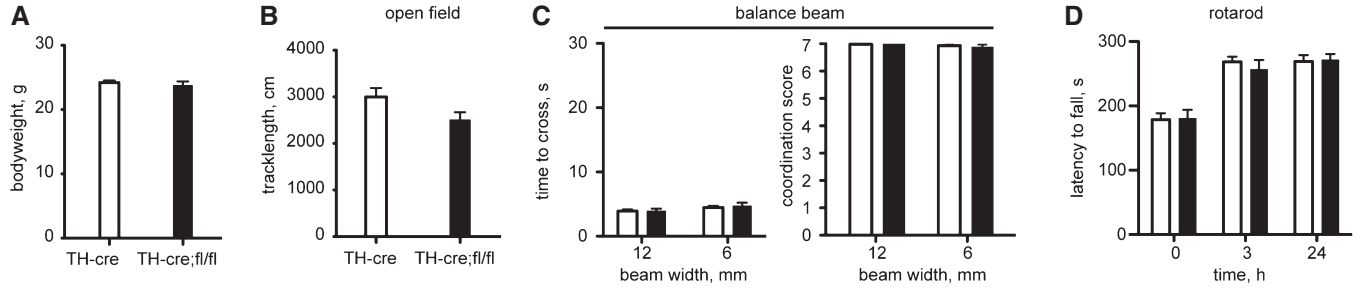

E

fore limbs

Parameter	Unit	p-value	mean TH-cre	mean TH-cre;fl/fl
MIDLINE.DISTANCE	(cm)	0.003 **	-2.914	-3.348
BRAKE	(s)	0.007 **	0.048	0.038
STANCE	(s)	0.012 *	0.142	0.126
OVERLAP.DISTANCE	(cm)	0.028 *	1.419	1.873
X.BRAKE.STRIDE	(%)	0.044 *	19.329	16.771
STRIDE	(s)	0.049 *	0.252	0.229
STRIDE.LENGTH	(cm)	0.057	6.300	5.736
STRIDE.FREQUENCY	(steps/s)	0.063	4.079	4.457
X.PROPEL.STANCE	(%)	0.073	65.743	69.636
X.BRAKE.STANCE	(%)	0.073	34.257	30.364
PAW.AREA.VAR	(cm^2)	0.086	0.016	0.020
ABS.AXIS.DISTANCE	(cm)	0.138	0.911	0.866
NORM.STRIDE.LENGTH	(real#)	0.167	0.553	0.488
MIN.DA.DT	(cm^2/s)	0.168	-4.522	-4.989
ABS.PAW.ANGLE	(deg)	0.235	10.493	7.557
NORM.STANCE.WIDTH	(real#)	0.282	0.438	0.416
STANCE.SWING	(real#)	0.293	1.307	1.221
PROPEL	(s)	0.319	0.093	0.088
SWING	(s)	0.333	0.110	0.103
PAW.AREA	(cm^2)	0.363	0.234	0.247
STANCE.WIDTH.CV	(CV%)	0.370	16.394	13.229
X.SWING.STRIDE	(%)	0.386	43.571	44.929
X.STANCE.STRIDE	(%)	0.390	56.429	55.079
FORELIMB.WEIGHT.SUPPORT		0.401	0.699	0.679
STANCE.WIDTH.VAR	(cm)	0.411	0.289	0.236
STRIDE.LENGTH.CV	(CV%)	0.415	12.004	13.201
STEP.ANGLE.CV	(CV%)	0.429	23.609	19.264
X.PROPEL.STRIDE	(%)	0.457	37.086	38.300
MAX.DA.DT	(cm^2/s)	0.538	15.366	16.048
STEP.ANGLE	(deg)	0.561	57.500	60.800
PAW.ANGLE.VAR	(deg)	0.643	8.721	9.379
STEP.ANGLE.VAR	(deg)	0.690	12.330	11.543
SWING.DURATION.CV	(CV%)	0.729	14.884	14.144
ATAXIA.COEFF	(real#)	0.772	0.404	0.418
PAW.ANGLE	(deg)	0.805	0.264	-0.300
STANCE.WIDTH	(cm)	0.805	1.771	1.800
STANCE.FACTOR	(real#)	0.808	1.003	1.009
GAIT.SYMMETRY	(real#)	0.853	1.004	1.003
STRIDE.LENGTH.VAR	(cm)	0.940	0.748	0.754
PPP	(cm)	0.975	0.506	0.508

hind limbs

Parameter	Unit	p-value	mean TH-cre	mean TH-cre;fl/fl
PAW.DRAG	(real#)	0.005 **	-5.160	-6.605
OVERLAP.DISTANCE	(cm)	0.028 *	1.419	1.873
PAW.WIDTH	(cm)	0.028 *	0.780	0.711
PAW.AREA	(cm^2)	0.030 *	0.584	0.531
MAX.DA.DT	(cm^2/s)	0.036 *	48.283	42.121
STANCE	(s)	0.042 *	0.156	0.145
PROPEL	(s)	0.047 *	0.121	0.103
STRIDE	(s)	0.047 *	0.252	0.229
STRIDE.LENGTH	(cm)	0.053	6.307	5.743
NORM.STANCE.WIDTH	(real#)	0.061	0.694	0.646
STEP.ANGLE.CV	(CV%)	0.070	22.617	33.913
STRIDE.FREQUENCY	(steps/s)	0.083	4.086	4.443
STEP.ANGLE	(deg)	0.084	56.657	47.100
SWING	(s)	0.111	0.097	0.085
STANCE.WIDTH.CV	(CV%)	0.148	5.950	7.143
PAW.LENGTH	(cm)	0.152	1.458	1.391
STEP.ANGLE.VAR	(deg)	0.160	12.530	14.960
NORM.STRIDE.LENGTH	(real#)	0.166	0.554	0.489
X.BRAKE.STRIDE	(%)	0.171	13.650	18.014
STANCE.WIDTH.VAR	(cm)	0.173	0.167	0.200
PAW.WIDTH.VAR	(cm)	0.174	0.051	0.044
X.BRAKE.STANCE	(%)	0.191	22.129	28.836
X.PROPEL.STANCE	(%)	0.191	77.871	71.164
BRAKE	(s)	0.272	0.034	0.042
PAW.LENGTH.VAR	(cm)	0.290	0.124	0.111
ABS.AXIS.DISTANCE	(cm)	0.323	1.461	1.390
X.SHARED.STANCE	(%)	0.336	33.736	37.736
STANCE.SWING	(real#)	0.344	1.636	1.743
X.PROPEL.STRIDE	(%)	0.381	48.193	45.114
X.STANCE.STRIDE	(%)	0.415	61.864	63.129
X.SWING.STRIDE	(%)	0.415	38.136	36.871
STRIDE.LENGTH.CV	(CV%)	0.484	12.006	13.413
SHARED.STANCE	(s)	0.603	0.052	0.055
SFI	(cm)	0.669	-8.795	-8.650
TFI	(cm)	0.674	-8.799	-8.661
MIDLINE.DISTANCE	(cm)	0.689	1.529	1.656
SWING.DURATION.CV	(CV%)	0.695	11.966	12.931
PAW.ANGLE.VAR	(deg)	0.698	4.164	4.343
TAU.PROPULSION	(real#)	0.707	0.161	0.148
STANCE.FACTOR	(real#)	0.753	1.033	1.024
MIN.DA.DT	(cm^2/s)	0.756	-8.642	-8.517
PFI	(cm)	0.797	-11.781	-12.079
ABS.PAW.ANGLE	(deg)	0.798	15.471	15.121
GAIT.SYMMETRY	(real#)	0.853	1.004	1.003
PAW.ANGLE	(deg)	0.928	0.929	0.807
ATAXIA.COEFF	(real#)	0.940	0.411	0.416
PPP	(cm)	0.975	0.506	0.508
STRIDE.LENGTH.VAR	(cm)	0.993	0.759	0.760
PAW.AREA.VAR	(cm^2)	1.000	0.036	0.036
STANCE.WIDTH	(cm)	1.000	2.800	2.800

Figure EV5. Loss of FBXO7 in TH$^+$ cells results in late-onset motor deficits.

A Average body weight of 2-month-old TH-Cre and TH-Cre;fl/fl mice. n = 15 and 9, respectively (unpaired t-test, mean ± s.e.m.).

B–D Open field test (B), balance beam test (time to cross and coordination score were measured, C), and rotarod (D) of 2-month-old TH-Cre and TH-Cre;fl/fl mice. n = 15 and 9, respectively (unpaired t-test or Mann–Whitney U-test (coordination score), mean ± s.e.m.).

E Parameters tested in DigiGait analysis (unpaired t-test, *$P < 0.05$, **$P < 0.01$, mean ± s.e.m.).